

EDINBURGH 96/4
May 1996

Next-to-Leading Corrections to the BFKL Equation

Vittorio Del Duca

*Particle Physics Theory Group, Dept. of Physics and Astronomy
University of Edinburgh, Edinburgh EH9 3JZ, Scotland, UK*

Abstract

Using the helicity formalism in the high-energy limit, we compute the amplitudes which generate the real next-to-leading-logarithmic corrections to the BFKL equation. Accordingly, we provide a list of all the off-shell vertices necessary to build such amplitudes.

*To appear in the Proceedings of
Les Rencontres de Physique de la Vallee d'Aoste
La Thuile, Val d'Aosta, Italy, March 1996*

1 Introduction

Semi-hard strong-interaction processes, for which the squared center-of-mass energy s is much larger than the momentum transfer Q^2 , have attracted a lot of interest in the latest years, because of the large kinematic region explored in deeply inelastic scattering (DIS) by the electron-proton collider at HERA, where values of $x_{bj} = Q^2/s$ of the order of 10^{-5} have been attained [1]. The evolution of the $F_2(x_{bj}, Q^2)$ structure function in $\ln(Q^2)$ is described by the Dokshitzer-Gribov-Lipatov-Altarelli-Parisi (DGLAP) equation to an accuracy determined by the order of α_s to which we compute the expansion of the splitting functions $P_{ab}(x, \alpha_s)$, with $a, b =$ quarks or gluons. At very small values of x_{bj} we may consider to resum the leading (logarithmic) contributions in $1/x$ to the splitting functions to all orders in α_s . This may be performed by using the Balitsky-Fadin-Kuraev-Lipatov (BFKL) evolution equation [2], which allows us to compute the gluon splitting functions at leading logarithmic (LL) accuracy in $1/x$ [3], and the quark splitting functions at next-to-leading logarithmic (NLL) accuracy [4]. In order to know the gluon splitting functions at NLL accuracy, the NLL corrections to the BFKL equation must be computed.

However, a caveat is in order: the BFKL equation computes the radiative corrections to parton-parton scattering in the high-energy limit, assuming that the outgoing partons are balanced in transverse momentum. Therefore only one hard transverse-momentum scale is allowed in the process. It is not possible to assess whether this is realized in the configurations that drive the rise of F_2 at small x_{bj} . Such a constraint, though, may be forced upon the DIS process at small x_{bj} by tagging a jet in the proton direction and by requiring that the squared jet transverse momentum is of the order of Q^2 [5]. An analogous process for which one may consider to resum the leading logarithms, in $\ln(\hat{s}/Q^2)$, in the partonic cross section is two-jet production at large rapidity intervals $\Delta\eta$ [6], a process which may be explored at the Tevatron $\bar{p}p$ collider. A comparison of the $\mathcal{O}(\alpha_s^3)$ matrix elements, exact and in the multi-Regge approximation used in the BFKL calculation, shows though that the discrepancies are quite big at the not very large values of $\Delta\eta$ attainable at the Tevatron, and would still be sizeable at the LHC collider [7]. This gives one more reason to compute the NLL corrections to the BFKL equation.

The working tools of the BFKL theory are the Fadin-Kuraev-Lipatov (FKL) multigluon amplitudes [8], [9] in the multi-Regge kinematics, which requires that the final-state partons are strongly ordered in rapidity and have comparable transverse momentum. The parton-parton scattering may be initiated by either quarks or gluons, however in the high-energy limit the leading contribution comes only from gluon exchange in the cross channel, therefore the leading corrections to parton-parton scattering are purely gluonic.

The building blocks of the tree-level FKL amplitudes are the process-dependent helicity-conserving vertices $g^* g \rightarrow g$, eq.(9) with g^* an off-shell gluon, and $g^* q \rightarrow q$, or $g^* \bar{q} \rightarrow \bar{q}$, eq.(12) and (15), which produce a parton at either end of the ladder; and the process-independent Lipatov vertex $g^* g^* \rightarrow g$, eq.(19), which emits a gluon along the ladder. The helicity-conserving and the Lipatov vertices, and accordingly the FKL amplitudes, assume a simpler analytic form when the helicity of the produced gluons is explicitly fixed [10], [11]. The LL virtual radiative corrections then *reggeize* the gluons, i.e. make the gluon propagators exchanged in the cross channel to assume a Regge-like form, eq.(??). The Lipatov vertex and the reggeized gluon enter the BFKL equation, and the helicity-conserving vertices fix the boundary conditions to it.

The NLL corrections to the FKL amplitudes are divided into real corrections, induced by the corrections to the multi-Regge kinematics [12]-[17], and virtual NLL corrections. The real corrections to the tree-level FKL amplitudes arise from the kinematical regions in which two partons are produced with similar rapidity, either at the ends of or along the ladder, termed the forward-rapidity and the central-rapidity regions respectively. The building blocks of these amplitudes are the vertices which describe the emission of two partons in the forward-rapidity region, $g^* g \rightarrow g g$ eq.(26), $g^* g \rightarrow \bar{q} q$ eq.(28), and $g^* q \rightarrow g q$ eq.(30) and (32); and in the central-rapidity region, $g^* g^* \rightarrow g g$ eq.(40) or $g^* g^* \rightarrow \bar{q} q$ eq.(44). The vertices for the emission in the central-rapidity region determine the real NLL corrections to the BFKL equation [14], and the vertices for the emission in the forward-rapidity region fix the boundary conditions to it. All vertices transform into their complex conjugates under helicity reversal.

2 Tree-level amplitudes in the helicity formalism

A tree-level multigluon amplitude in a helicity basis has the form [18]

$$M_n = \sum_{[a,1,\dots,n,b]'} \text{tr}(\lambda^a \lambda^{d_1} \dots \lambda^{d_n} \lambda^b) m(-p_a, -\nu_a; p_1, \nu_1; \dots; p_n, \nu_n; -p_b, -\nu_b), \quad (1)$$

where a, d_1, \dots, d_n, b , and $\nu_a, \nu_1, \dots, \nu_b$ are respectively the colors and the helicities of the gluons, the λ 's are the color matrices in the fundamental representation of $SU(N_c)$, the sum is over the noncyclic permutations of the color orderings $[a, 1, \dots, b]$ and all the momenta are taken as outgoing. For the *maximally helicity-violating* configurations $(-, -, +, \dots, +)$, the subamplitudes $m(-p_a, -\nu_a; p_1, \nu_1; \dots; p_n, \nu_n; -p_b, -\nu_b)$, invariant with respect to tran-

formations between physical gauges, assume the form [19],

$$m(-, -, +, \dots, +) = 2^{1+n/2} g^n \frac{\langle p_i p_j \rangle^4}{\langle p_a p_1 \rangle \cdots \langle p_n p_b \rangle \langle p_b p_a \rangle}, \quad (2)$$

with i and j the gluons of negative helicity, and with the spinor products defined as

$$\begin{aligned} \langle pk \rangle &= \langle p - | k + \rangle = \overline{\psi_-(p)} \psi_+(k), \\ [pk] &= \langle p + | k - \rangle = \overline{\psi_+(p)} \psi_-(k), \end{aligned} \quad (3)$$

through massless Dirac spinors of fixed helicity, $\psi_{\pm}(p)$. The subamplitudes (2) are *exact*, and in computing them the representation

$$\epsilon_{\mu}^{\pm}(p, k) = \pm \frac{\langle p \pm | \gamma_{\mu} | k \pm \rangle}{\sqrt{2} \langle k \mp | p \pm \rangle}, \quad (4)$$

for the gluon polarization has been used, with k an arbitrary light-like momentum. The ordering of the spinor products in the denominator of eq.(2) is set by the permutation of the color ordering $[a, 1, \dots, b]$. The configurations $(+, +, -, \dots, -)$ are then obtained by replacing the $\langle pk \rangle$ products with $[kp]$ products.

A tree-level multigluon amplitude with a quark-antiquark pair has the form [18],

$$M_n = \sum_{[1, \dots, n]} (\lambda^{d_1} \cdots \lambda^{d_n})_{i\bar{j}} m(q, \nu; p_1, \nu_1; \dots; p_n, \nu_n; \bar{q}, -\nu), \quad (5)$$

where (i, \bar{j}) are the color indices of the quark-antiquark pair, the sum is over the permutations of the color orderings $[1, \dots, n]$, and we have taken into account that helicity is conserved over the quark line. For the *maximally helicity-violating* configurations, $(-, -, +, \dots, +)$, the subamplitudes are

$$\begin{aligned} m(\bar{q}^+; q^-; g_1; \dots; g_n) &= 2^{n/2} g^n \frac{\langle \bar{q} p_i \rangle \langle q p_i \rangle^3}{\langle \bar{q} q \rangle \langle q p_1 \rangle \cdots \langle p_n \bar{q} \rangle} \\ m(\bar{q}^-; q^+; g_1; \dots; g_n) &= 2^{n/2} g^n \frac{\langle \bar{q} p_i \rangle^3 \langle q p_i \rangle}{\langle \bar{q} q \rangle \langle q p_1 \rangle \cdots \langle p_n \bar{q} \rangle}, \end{aligned} \quad (6)$$

where the i^{th} gluon has negative helicity, and the ordering of the spinor products in the denominator is set by the permutation of the color ordering $[1, \dots, n]$. The subamplitudes (2) and (6) are related by a supersymmetric Ward identity [18].

3 Amplitudes in the multi-Regge kinematics

We consider the elastic scattering of two gluons of momenta p_a and p_b in two gluons of momenta $p_{a'}$ and $p_{b'}$, in the high-energy limit $\hat{s} \gg |\hat{t}|$ (Fig. 1a). Let y be the rapidity difference between the outgoing gluons, and $p_{b'\perp} = -p_{a'\perp} = q_\perp$. Then $\hat{t} \simeq -|q_\perp|^2$, and $\hat{s} \simeq -\hat{t}e^y$, and the high-energy limit implies that $y \gg 1$. Using eq.(2) and the spinor products in the representation of ref. [11], and rewriting the traces of λ matrices as products of structure constants,

$$[\lambda^a, \lambda^b] = i f^{abc} \lambda^c, \quad \text{tr}(\lambda^a \lambda^b) = \frac{\delta_{ab}}{2}, \quad (7)$$

the scattering amplitude in the high-energy limit may be written as,

$$M_{\nu_a \nu_{a'} \nu_{b'} \nu_b}^{aa'bb'} = 2\hat{s} \left[ig f^{aa'c} C_{-\nu_a \nu_{a'}}^{gg}(-p_a, p_{a'}) \right] \frac{1}{\hat{t}} \left[ig f^{bb'c} C_{-\nu_b \nu_{b'}}^{gg}(-p_b, p_{b'}) \right], \quad (8)$$

with the helicity-conserving vertices $g^* g \rightarrow g$, with g^* an off-shell gluon, [9], [11]

$$C_{-+}^{gg}(-p_a, p_{a'}) = 1 \quad C_{-+}^{gg}(-p_b, p_{b'}) = \frac{p_{b'\perp}^*}{p_{b'\perp}}, \quad (9)$$

where we use the complex notation, $p_\perp = p_x + ip_y$, for the transverse momentum. The C -vertices transform into their complex conjugates under helicity reversal, $C_{\{\nu\}}^*(\{k\}) = C_{\{-\nu\}}(\{k\})$. The helicity-flip vertex C_{++} is subleading in the high-energy limit. Using

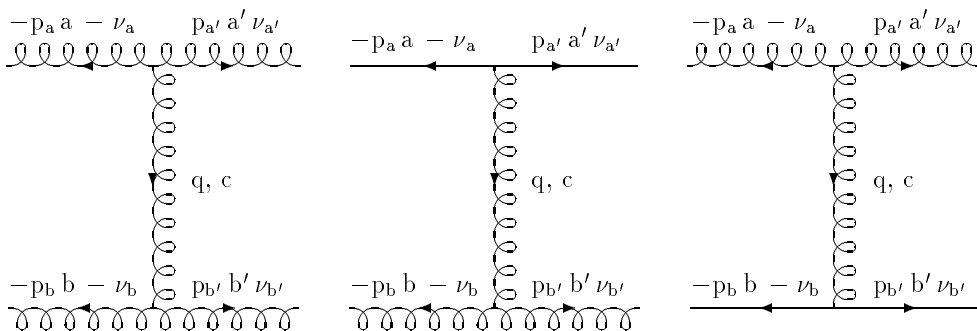


Figure 1: (a) Amplitude for $gg \rightarrow gg$ scattering and (b), (c) for $qg \rightarrow qg$ scattering. We label the external lines with momentum, always taken as outgoing, color and helicity, and the internal lines with momentum and color.

eq.(5-7), the quark-gluon $qg \rightarrow qg$ scattering amplitude in the high-energy limit is,

$$M^{qg \rightarrow qg} = 2\hat{s} \left[g \lambda_{a'\bar{a}}^c C_{-\nu_a \nu_a}^{\bar{q}q}(-p_a, p_{a'}) \right] \frac{1}{\hat{t}} \left[ig f^{bb'c} C_{-\nu_b \nu_{b'}}^{gg}(-p_b, p_{b'}) \right], \quad (10)$$

$$M^{gq \rightarrow gq} = 2\hat{s} \left[ig f^{aa'c} C_{-\nu_a \nu_{a'}}^{gg}(-p_a, p_{a'}) \right] \frac{1}{\hat{t}} \left[g \lambda_{b'\bar{b}}^c C_{-\nu_b \nu_b}^{\bar{q}q}(-p_b, p_{b'}) \right], \quad (11)$$

where the antiquark is $-p_a$ in eq.(10) (Fig. 1b) and $-p_b$ in eq.(11) (Fig. 1c), and the C -vertices $g^* q \rightarrow q$ are,

$$C_{-+}^{\bar{q}q}(-p_a, p_{a'}) = 1; \quad C_{-+}^{\bar{q}q}(-p_b, p_{b'}) = \left(\frac{p_{b'\perp}^*}{p_{b'\perp}} \right)^{1/2}. \quad (12)$$

Analogously, the antiquark-gluon $\bar{q} g \rightarrow \bar{q} g$ scattering amplitude is,

$$M^{\bar{q}g \rightarrow \bar{q}g} = 2\hat{s} \left[g \lambda_{a\bar{a}'}^c C_{-\nu_a\nu_a}^{q\bar{q}}(-p_a, p_{a'}) \right] \frac{1}{\hat{t}} \left[ig f^{bb'c} C_{-\nu_b\nu_b}^{gg}(-p_b, p_{b'}) \right], \quad (13)$$

$$M^{g\bar{q} \rightarrow g\bar{q}} = 2\hat{s} \left[ig f^{aa'c} C_{-\nu_a\nu_a}^{gg}(-p_a, p_{a'}) \right] \frac{1}{\hat{t}} \left[g \lambda_{b\bar{b}'}^c C_{-\nu_b\nu_b}^{q\bar{q}}(-p_b, p_{b'}) \right], \quad (14)$$

where the antiquark is $p_{a'}$ in eq.(13) (Fig. 1b) and $p_{b'}$ in eq.(14) (Fig. 1c), and the C -vertices $g^* \bar{q} \rightarrow \bar{q}$ are,

$$C_{-+}^{q\bar{q}}(-p_a, p_{a'}) = -1; \quad C_{-+}^{q\bar{q}}(-p_b, p_{b'}) = - \left(\frac{p_{b'\perp}^*}{p_{b'\perp}} \right)^{1/2}. \quad (15)$$

In the amplitudes (8), (10), (11), (13), (14), the leading contributions from all the Feynman diagrams have been included. However, the amplitudes have the effective form of a gluon exchange in the t channel (Fig. 1), and differ only for the relative color strength in the production vertices [20]. This allows us to replace an incoming gluon with a quark, for instance on the upper line, via the simple substitution

$$ig f^{aa'c} C_{-\nu_a\nu_a}^{gg}(-p_a, p_{a'}) \leftrightarrow g \lambda_{a\bar{a}'}^c C_{-\nu_a\nu_a}^{q\bar{q}}(-p_a, p_{a'}), \quad (16)$$

and similar ones for an antiquark and/or for the lower line.

Next, we consider the production of three gluons of momenta $p_{a'}$, k and $p_{b'}$ (Fig. 2a), and we require that the gluons are strongly ordered in their rapidities and have comparable transverse momenta,

$$y_{a'} \gg y \gg y_{b'}; \quad |p_{a'\perp}| \simeq |k_\perp| \simeq |p_{b'\perp}|. \quad (17)$$

Eq.(17) is the simplest example of *multi-Regge kinematics*. Using eq.(2) and the algebra (7), the scattering amplitude is,

$$\begin{aligned} M^{gg \rightarrow ggg} &= 2\hat{s} \left[ig f^{aa'c} C_{-\nu_a\nu_a}^{gg}(-p_a, p_{a'}) \right] \frac{1}{\hat{t}_1} \\ &\times \left[ig f^{cd'c'} C_{\nu'}^g(q_1, q_2) \right] \frac{1}{\hat{t}_2} \left[ig f^{bb'c'} C_{-\nu_b\nu_b}^{gg}(-p_b, p_{b'}) \right], \end{aligned} \quad (18)$$

with $p_{a'\perp} = -q_{1\perp}$, $p_{b'\perp} = q_{2\perp}$ and $\hat{t}_i \simeq -|q_{i\perp}|^2$ with $i = 1, 2$ and with the Lipatov vertex $g^* g^* \rightarrow g$ [8], [10], [11],

$$C_+^g(q_1, q_2) = \sqrt{2} \frac{q_{1\perp}^* q_{2\perp}}{k_\perp}. \quad (19)$$

The amplitude (18) has the effective form of a gluon-ladder exchange in the t channel, however the additional gluon k has been inserted either along the ladder (Fig. 2a) or as a bremsstrahlung gluon on the external legs. In this sense the Lipatov vertex (19) is a non-local effective vertex. Again, we may replace an incoming gluon with a quark via the substitution (16).

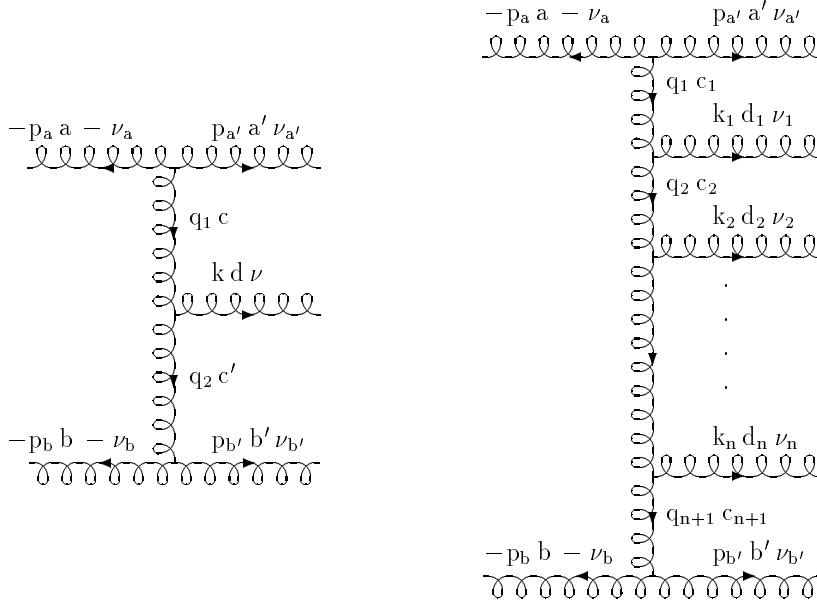


Figure 2: (a) Amplitude for $gg \rightarrow ggg$ scattering, and (b) for the production of $n + 2$ gluons.

Eq.(18) generalizes to the production of $n + 2$ gluons [9] (Fig. 2b) in the multi-Regge kinematics,

$$y_{a'} \gg y_1 \gg \dots \gg y_n \gg y_{b'}; \quad |p_{i\perp}| \simeq |p_\perp|, \quad (20)$$

with $i = a', 1, \dots, n, b'$ in a straightforward manner,

$$\begin{aligned} M_{\nu_a \nu_{a'} \nu_1 \dots \nu_n \nu_{b'} \nu_b}^{aa' d_1 \dots d_n b' b} &= 2\hat{s} \left[ig f^{aa' c_1} C_{-\nu_a \nu_{a'}}^{gg}(-p_a, p_{a'}) \right] \frac{1}{\hat{t}_1} \\ &\times \left[ig f^{c_1 d_1 c_2} C_{\nu_1}^g(q_1, q_2) \right] \frac{1}{\hat{t}_2} \\ &\times \end{aligned} \quad (21)$$

$$\begin{aligned}
& \times \\
& \times \left[ig f^{c_n d_n c_{n+1}} C_{\nu_n}^{gg} (q_n, q_{n+1}) \right] \frac{1}{\hat{t}_{n+1}} \\
& \times \left[ig f^{bb' c_{n+1}} C_{-\nu_b \nu_{b'}}^{gg} (-p_b, p_{b'}) \right],
\end{aligned}$$

with $\hat{t}_i \simeq -|q_{i\perp}|^2$ and $i = 1, \dots, n+1$. Thus the tree-level FKL amplitudes are built by repeatedly using the process-independent Lipatov vertex (19) for the gluon emission along the ladder, and are bounded by process-dependent outer vertices, which for gluons are given by eq.(9) and for (anti)quarks by eq.(12) and (15). However, no quarks may be produced along the ladder since that would involve quark exchange in the t channel, which is suppressed in the kinematics (20).

4 Amplitudes in next-to-leading approximation

In order to obtain amplitudes in next-to-leading approximation, we must relax the strong rapidity ordering between the produced gluons (20), and allow for the production of two gluons or of a $q\bar{q}$ pair with similar rapidity.

4.1 The forward-rapidity region

We begin with the simplest case, i.e. the production of three partons of momenta k_1 , k_2 and $p_{b'}$ in the scattering between two partons of momenta p_a and p_b , with partons k_1 and k_2 in the forward-rapidity region of parton p_a ,

$$y_1 \simeq y_2 \gg y_{b'}; \quad |k_{1\perp}| \simeq |k_{2\perp}| \simeq |p_{b'\perp}|. \quad (22)$$

First we consider the amplitude for the scattering $gg \rightarrow ggg$ (Fig. 3a) [12], [13]. Using eq.(2) we obtain

$$\begin{aligned}
& M^{gg}(-p_a, -\nu_a; k_1, \nu_1; k_2, \nu_2; p_{b'}, \nu_{b'}; -p_b, -\nu_b) \\
& = 2\sqrt{2} g^3 \frac{\hat{s}}{|p_{b'\perp}|^2} C_{-\nu_b \nu_{b'}}^{gg}(-p_b, p_{b'}) C_{-\nu_a \nu_1 \nu_2}^{ggg}(-p_a, k_1, k_2) \{ A_{\Sigma \nu_i}(-p_a, k_1, k_2) \\
& \times \text{tr} \left(\lambda^a \lambda^{d_1} \lambda^{d_2} \lambda^{b'} \lambda^b - \lambda^a \lambda^{d_1} \lambda^{d_2} \lambda^b \lambda^{b'} + \lambda^a \lambda^{b'} \lambda^b \lambda^{d_2} \lambda^{d_1} - \lambda^a \lambda^b \lambda^{b'} \lambda^{d_2} \lambda^{d_1} \right) \\
& - B_{\Sigma \nu_i}(-p_a, k_1, k_2) \text{tr} \left(\lambda^a \lambda^{d_1} \lambda^{b'} \lambda^b \lambda^{d_2} - \lambda^a \lambda^{d_2} \lambda^b \lambda^{b'} \lambda^{d_1} \right) + \left(\begin{array}{l} k_1 \leftrightarrow k_2 \\ d_1 \leftrightarrow d_2 \end{array} \right) \}, \quad (23)
\end{aligned}$$

with the vertex $C_{-\nu_b\nu_{b'}}^{gg}(-p_b, p_{b'})$ as in eq.(9), $\sum \nu_i = -\nu_a + \nu_1 + \nu_2$ and,

$$C_{-++}^{ggg}(-p_a, k_1, k_2) = 1; \quad C_{+--+}^{ggg}(-p_a, k_1, k_2) = \frac{1}{\left(1 + \frac{k_2^+}{k_1^+}\right)^2}; \quad (24)$$

$$C_{+++}^{ggg}(-p_a, k_1, k_2) = \frac{1}{\left(1 + \frac{k_1^+}{k_2^+}\right)^2}; \quad A_+(-p_a, k_1, k_2) = 2 \frac{p_{b'\perp}}{k_{1\perp}} \frac{1}{k_{2\perp} - k_{1\perp} \frac{k_2^+}{k_1^+}};$$

$$B_{\Sigma\nu_i}(-p_a, k_1, k_2) = A_{\Sigma\nu_i}(-p_a, k_1, k_2) + A_{\Sigma\nu_i}(-p_a, k_2, k_1), \quad (25)$$

with the production vertex of gluons k_1 and k_2 given by the product of the vertex $C^{ggg}(-p_a, k_1, k_2)$ with either A or B , where we have used light-cone coordinates $k^\pm = k_0 \pm k_z$. The vertex $C_{+++}^{ggg}(-p_a, k_1, k_2)$ is subleading to the required accuracy. The vertex $A_{\Sigma\nu_i}$ has a collinear divergence as $2k_1 \cdot k_2 \rightarrow 0$, but the divergence cancels out in the vertex $B_{\Sigma\nu_i}$ where gluons 1 and 2 are not adjacent in color ordering [13]. Using the algebra (7) and eq.(25), and fixing $\hat{t} \simeq -|p_{b'\perp}|^2$, the amplitude (23) may be rewritten as,

$$M^{gg}(-p_a, -\nu_a; k_1, \nu_1; k_2, \nu_2; p_{b'}, \nu_{b'}; -p_b, -\nu_b) \quad (26)$$

$$= 2\hat{s} \left\{ C_{-\nu_a\nu_1\nu_2}^{ggg}(-p_a, k_1, k_2) \left[(ig)^2 f^{ad_1c} f^{cd_2c'} \frac{1}{\sqrt{2}} A_{\Sigma\nu_i}(-p_a, k_1, k_2) + \left(\begin{array}{c} k_1 \leftrightarrow k_2 \\ d_1 \leftrightarrow d_2 \end{array} \right) \right] \right\}$$

$$\times \frac{1}{\hat{t}} \left[ig f^{bb'c'} C_{-\nu_b\nu_{b'}}^{gg}(-p_b, p_{b'}) \right],$$

where we have enclosed the production vertex $g^* g \rightarrow gg$ of gluons k_1 and k_2 in curly brackets. In the multi-Regge limit $k_1^+ \gg k_2^+$ it becomes

$$\lim_{k_1^+ \gg k_2^+} \frac{1}{\sqrt{2}} C_{-\nu_a\nu_1\nu_2}^{ggg}(-p_a, k_1, k_2) A_{\Sigma\nu_i}(-p_a, k_1, k_2) = C_{-\nu_a\nu_1}^{gg}(-p_a, k_1) \frac{1}{\hat{t}_{12}} C_{\nu_2}^g(q_{12}, q), \quad (27)$$

with q_{12} the momentum of the gluon exchanged between k_1 and k_2 in the multi-Regge limit, and $\hat{t}_{12} \simeq -|q_{12\perp}|^2$; thus the amplitude (26) reduces to eq.(18), as expected.

Using eq.(5-7), the amplitude for the production of a $q\bar{q}$ pair in the forward-rapidity region of gluon p_a is (Fig. 3b), [16], [17],

$$M^{\bar{q}q}(-p_a, -\nu_a; k_1, \nu_1; k_2, -\nu_1; p_{b'}, \nu_{b'}; -p_b, -\nu_b) \quad (28)$$

$$= 2\hat{s} \left\{ \sqrt{2} g^2 C_{-\nu_a\nu_1-\nu_1}^{g\bar{q}q}(-p_a, k_1, k_2) \left[\left(\lambda^{c'} \lambda^a \right)_{d_2\bar{d}_1} A_{-\nu_a}(k_1, k_2) + \left(\lambda^a \lambda^{c'} \right)_{d_2\bar{d}_1} A_{-\nu_a}(k_2, k_1) \right] \right\}$$

$$\times \frac{1}{\hat{t}} \left[ig f^{bb'c'} C_{-\nu_b\nu_{b'}}^{gg}(-p_b, p_{b'}) \right],$$

with k_1 the antiquark, the production vertex $g^* g \rightarrow \bar{q} q$ in curly brackets, A defined in eq.(24), and $C^{g\bar{q}q}$ given by,

$$C_{++-}^{g\bar{q}q}(-p_a, k_1, k_2) = \frac{1}{2} \sqrt{\frac{k_1^+}{k_2^+}} \frac{1}{\left(1 + \frac{k_1^+}{k_2^+}\right)^2} \quad (29)$$

$$C_{+-+}^{g\bar{q}q}(-p_a, k_1, k_2) = \frac{1}{2} \sqrt{\frac{k_2^+}{k_1^+}} \frac{1}{\left(1 + \frac{k_2^+}{k_1^+}\right)^2}.$$

Note that the vertex $B_{\Sigma\nu_i}$ (25) does not appear in eq.(28) because the $\bar{q} q$ pair is bound to

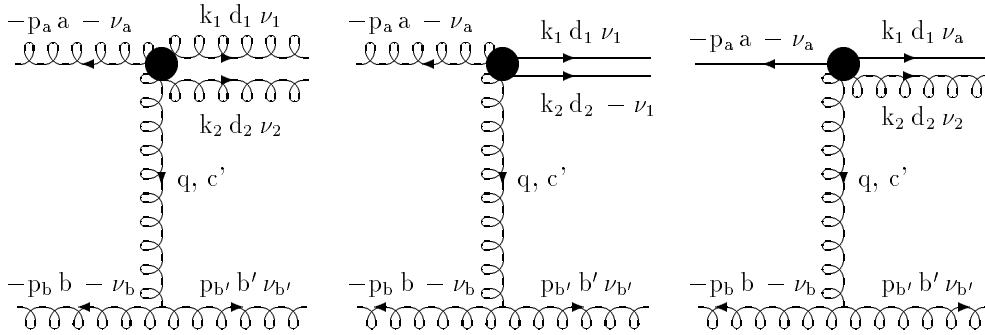


Figure 3: Amplitudes for the production of three partons, with partons k_1 and k_2 in the forward-rapidity region of parton k_0 .

be adjacent in color ordering [cf. eq.(5)]. In the multi-Regge limit $k_1^+ \gg k_2^+$ the vertices (29) vanish, in agreement with the remark at the end of sect. 3.

Using again eq.(5-7), the amplitude for the production of a qg pair in the forward-rapidity region of quark p_a is (Fig. 3c),

$$M^{\bar{q}q}(-p_a, -\nu_a; k_1, \nu_a; k_2, \nu_2; p_b', \nu_b'; -p_b, -\nu_b) \quad (30)$$

$$= 2\hat{s} \left\{ \sqrt{2} g^2 C_{-\nu_a\nu_a\nu_2}^{\bar{q}qg}(-p_a, k_1, k_2) \left[\left(\lambda^{d_2} \lambda^{c'}\right)_{d_1\bar{a}} A_{\nu_2}(k_1, k_2) - \left(\lambda^{c'} \lambda^{d_2}\right)_{d_1\bar{a}} B_{\nu_2}(k_1, k_2) \right] \right\}$$

$$\times \frac{1}{\hat{t}} \left[ig f^{bb'c'} C_{-\nu_b\nu_b'}^{gg}(-p_b, p_b') \right],$$

with $-p_a$ the antiquark, the production vertex $qg^* \rightarrow qg$ in curly brackets, A and B defined in eq.(24) and (25), and

$$C_{-++}^{\bar{q}qg}(-p_a, k_1, k_2) = \frac{1}{2} \frac{1}{\left(1 + \frac{k_2^+}{k_1^+}\right)^{1/2}}, \quad (31)$$

$$C_{+-+}^{\bar{q}qg}(-p_a, k_1, k_2) = \frac{1}{2} \frac{1}{\left(1 + \frac{k_2^+}{k_1^+}\right)^{3/2}}.$$

Analogously, when k_1 is the antiquark we obtain,

$$\begin{aligned} & M^{q\bar{q}}(-p_a, -\nu_a; k_1, \nu_a; k_2, \nu_2; p_{b'}, \nu_{b'}; -p_b, -\nu_b) \quad (32) \\ &= -2\hat{s} \left\{ \sqrt{2} g^2 C_{-\nu_a\nu_a\nu_2}^{q\bar{q}g}(-p_a, k_1, k_2) \left[(\lambda^{c'} \lambda^{d_2})_{ad_1} A_{\nu_2}(k_1, k_2) - (\lambda^{d_2} \lambda^{c'})_{ad_1} B_{\nu_2}(k_1, k_2) \right] \right\} \\ &\times \frac{1}{\hat{t}} \left[ig f^{bb'c'} C_{-\nu_b\nu_{b'}}^{gg}(-p_b, p_{b'}) \right], \end{aligned}$$

with

$$\begin{aligned} C_{-+++}^{q\bar{q}g}(-p_a, k_1, k_2) &= -\frac{1}{2} \frac{1}{\left(1 + \frac{k_2^+}{k_1^+}\right)^{1/2}}, \quad (33) \\ C_{+-+}^{q\bar{q}g}(-p_a, k_1, k_2) &= -\frac{1}{2} \frac{1}{\left(1 + \frac{k_2^+}{k_1^+}\right)^{3/2}}. \end{aligned}$$

In the multi-Regge limit $k_1^+ \gg k_2^+$ the amplitudes (30) and (32) reduce to eq.(18), with the substitution (16) for the upper line, and respectively the vertices $C^{q\bar{q}}$, eq.(12), and $C^{q\bar{q}}$, eq.(15). Finally, the amplitudes of Fig. 3 with a quark in the lower line are obtained via the corresponding substitution (16).

4.2 The central-rapidity region

We consider the production of four partons with momenta $p_{a'}$, k_1 , k_2 and $p_{b'}$, in the scattering between two partons of momenta p_a and p_b . We require that partons k_1 and k_2 have similar rapidity and are separated through large rapidity intervals from the partons emitted in the forward-rapidity regions, with all of them having comparable transverse momenta (Fig.4)

$$y'_A \gg y_1 \simeq y_2 \gg y'_B; \quad |k_{1\perp}| \simeq |k_{2\perp}| \simeq |p'_{A\perp}| \simeq |p'_{B\perp}|. \quad (34)$$

First we consider the amplitude for the scattering $gg \rightarrow gggg$ [12]-[14] (Fig.4a). Using eq.(2) and the amplitudes with three negative-helicity gluons [21], we have [13]

$$\begin{aligned} & M^{gg}(-p_a, -\nu_a; p_{a'}, \nu_{a'}; k_1, \nu_1; k_2, \nu_2; p_{b'}, \nu_{b'}; -p_b, -\nu_b) \quad (35) \\ &= -4g^4 \frac{\hat{s}}{|p_{a'\perp}|^2 |p_{b'\perp}|^2} C_{-\nu_a\nu_{a'}}^{gg}(-p_a, p_{a'}) C_{-\nu_b\nu_{b'}}^{gg}(-p_b, p_{b'}) \end{aligned}$$

$$\begin{aligned}
& \times \left\{ A_{\nu_1\nu_2}^{gg}(k_1, k_2) \left[\text{tr} \left(\lambda^a \lambda^{a'} \lambda^{d_1} \lambda^{d_2} \lambda^{b'} \lambda^b - \lambda^a \lambda^{a'} \lambda^{d_1} \lambda^{d_2} \lambda^b \lambda^{b'} \right. \right. \right. \\
& \left. \left. \left. - \lambda^a \lambda^{d_1} \lambda^{d_2} \lambda^{b'} \lambda^b \lambda^{a'} + \lambda^a \lambda^{d_1} \lambda^{d_2} \lambda^b \lambda^{b'} \lambda^{a'} \right) + \text{traces in reverse order} \right] - B_{\nu_1\nu_2}^{gg}(k_1, k_2) \right. \\
& \left. \times \left[\text{tr} \left(\lambda^a \lambda^{a'} \lambda^{d_1} \lambda^{b'} \lambda^b \lambda^{d_2} - \lambda^a \lambda^{a'} \lambda^{d_1} \lambda^b \lambda^{b'} \lambda^{d_2} \right) + \text{traces in reverse order} \right] + \begin{pmatrix} k_1 \leftrightarrow k_2 \\ \nu_1 \leftrightarrow \nu_2 \\ d_1 \leftrightarrow d_2 \end{pmatrix} \right\},
\end{aligned}$$

with the production vertices C of gluons $p_{a'}$ and $p_{b'}$ determined by eq.(9), and the vertex for the production of gluons k_1 and k_2 , $g^* g^* \rightarrow gg$, given by

$$B_{\nu_1\nu_2}^{gg}(k_1, k_2) = A_{\nu_1\nu_2}^{gg}(k_1, k_2) + A_{\nu_2\nu_1}^{gg}(k_2, k_1), \quad (36)$$

$$A_{++}^{gg}(k_1, k_2) = 2 \frac{p_{a'\perp}^* p_{b'\perp}}{k_{1\perp} k_{2\perp} - k_{1\perp} \frac{k_2^+}{k_1^+}},$$

$$\begin{aligned}
A_{+-}^{gg}(k_1, k_2) &= -2 \frac{k_{1\perp}^*}{k_{1\perp}} \left\{ -\frac{1}{\hat{s}_{12}} \left[\frac{k_{2\perp}^2 |q_{a\perp}|^2}{(k_1^- + k_2^-) k_2^+} + \frac{k_{1\perp}^2 |q_{b\perp}|^2}{(k_1^+ + k_2^+) k_1^-} + \frac{\hat{t} k_{1\perp} k_{2\perp}}{k_1^- k_2^+} \right] \right. \\
& \left. + \frac{(q_{b\perp} + k_{2\perp})^2}{\hat{t}} - \frac{q_{b\perp} + k_{2\perp}}{\hat{s}_{12}} \left[\frac{k_1^- + k_2^-}{k_1^-} k_{1\perp} - \frac{k_1^+ + k_2^+}{k_2^+} k_{2\perp} \right] \right\} \quad (37)
\end{aligned}$$

$$\begin{aligned}
\text{with} \quad & q_a = -(p_{a'} - p_a) \quad q_b = p_{b'} - p_b \\
\text{and} \quad & \hat{s}_{12} = 2k_1 \cdot k_2 \quad \hat{t} \simeq -(|q_{b\perp} + k_{2\perp}|^2 + k_1^- k_2^+).
\end{aligned}$$

Note that for equal helicities the vertices A and B are similar in form to the respective vertices in eq.(24) and (25), because the helicity structure of the amplitudes they belong to is similar. As in sect. 4.1, the vertex $A_{\nu_1\nu_2}^{gg}$ has a collinear divergence as $\hat{s}_{12} \rightarrow 0$, but the divergence cancels out in the vertex $B_{\nu_1\nu_2}^{gg}$. In addition, the amplitude (35) must not diverge more rapidly than $1/|q_{i\perp}|$ in the collinear regions $|q_{i\perp}| \rightarrow 0$, with $i = a, b$, in order for the related cross section not to diverge more than logarithmically [12]. Since eq.(35) has the poles $|q_{a\perp}|^2$ and $|q_{b\perp}|^2$, the A -vertex must be at least linear in $|q_{i\perp}|$,

$$\lim_{|q_{i\perp}| \rightarrow 0} A_{\nu_1\nu_2}^{gg}(k_1, k_2) = O(|q_{i\perp}|), \quad (38)$$

which is fulfilled by eq.(37). Finally, in the soft limit $k_1 \rightarrow 0$ we obtain

$$\lim_{k_1 \rightarrow 0} A_{+-}^{gg}(k_1, k_2) = \frac{q_{a\perp} q_{b\perp}^* k_{2\perp}}{q_{a\perp}^* q_{b\perp} k_{2\perp}^*} A_{++}^{gg}(k_1, k_2), \quad (39)$$

which, when integrated over the phase space of gluon k_1 , yields a logarithmic infrared divergence. Using the algebra (7) and eq.(36), and fixing $\hat{t}_i \simeq -|q_{i\perp}|^2$ with $i = a, b$, the

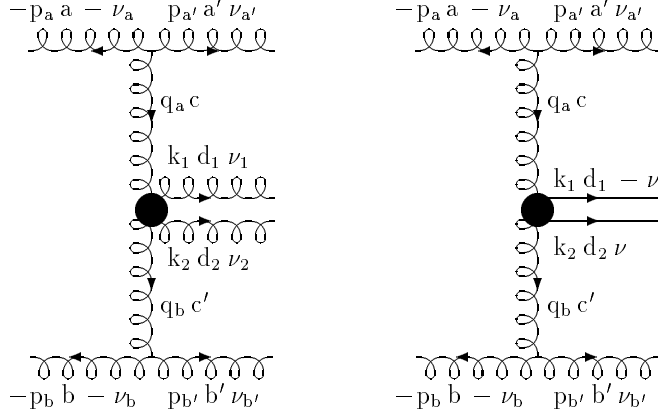


Figure 4: Amplitudes for the production of four partons, with partons k_1 and k_2 in the central-rapidity region.

amplitude (35) may be rewritten as

$$\begin{aligned}
& M^{gg}(-p_a, -\nu_a; p_{a'}, \nu_{a'}; k_1, \nu_1; k_2, \nu_2; p_{b'}, \nu_{b'}; -p_b, -\nu_b) \\
&= 2 \hat{s} \left[ig f^{aa'c} C_{-\nu_a \nu_{a'}}^{gg}(-p_a, p_{a'}) \right] \frac{1}{\hat{t}_a} \left\{ (ig)^2 f^{cd_1 e} f^{ed_2 c'} A_{\nu_1 \nu_2}^{gg}(k_1, k_2) + \left(\begin{array}{l} k_1 \leftrightarrow k_2 \\ \nu_1 \leftrightarrow \nu_2 \\ d_1 \leftrightarrow d_2 \end{array} \right) \right\} \\
&\times \frac{1}{\hat{t}_b} \left[ig f^{bb'c'} C_{-\nu_b \nu_{b'}}^{gg}(-p_b, p_{b'}) \right],
\end{aligned} \tag{40}$$

where we have enclosed the production vertex $g^* g^* \rightarrow gg$ of gluons k_1 and k_2 in curly brackets. In the multi-Regge limit $k_1^+ \gg k_2^+$ it becomes

$$\lim_{k_1^+ \gg k_2^+} A_{\nu_1 \nu_2}^{gg}(k_1, k_2) = C_{\nu_1}^g(q_a, q_{12}) \frac{1}{\hat{t}_{12}} C_{\nu_2}^g(q_{12}, q_b), \tag{41}$$

with q_{12} the momentum of the gluon exchanged between k_1 and k_2 and $\hat{t}_{12} \simeq -|q_{12\perp}|^2$; thus the amplitude (40) reduces to eq.(21), with $n = 2$. Finally, we note that fixing

$$\begin{aligned}
x &= \frac{k_1^+}{k_1^+ + k_2^+}, & \Delta_\perp &= k_{1\perp} + k_{2\perp}, & k_{2\perp} - k_{1\perp} \frac{k_2^+}{k_1^+} &= \frac{x\Delta_\perp - k_{1\perp}}{x}, \\
\hat{s}_{12} &= \frac{|k_{1\perp} - x\Delta_\perp|^2}{x(1-x)}, & \hat{t} &= -\frac{|k_{1\perp} - xq_{a\perp}|^2 + x(1-x)|q_{a\perp}|^2}{x},
\end{aligned} \tag{42}$$

the A-vertex (37) may be rewritten as [14],

$$A_{++}^{gg}(k_1, k_2) = -2 \frac{q_{a\perp}^* q_{b\perp}}{k_{1\perp}} \frac{x}{x\Delta_\perp - k_{1\perp}},$$

$$\begin{aligned}
A_{+-}^{gg}(k_1, k_2) &= -2 \frac{k_{1\perp}^*}{k_{1\perp}} \left[\frac{(q_{b\perp} + k_{2\perp})^2}{\hat{t}} + \frac{x|q_{a\perp}|^2 k_{2\perp}^2}{|\Delta_\perp|^2 (|k_{1\perp} - x\Delta_\perp|^2 + x(1-x)|\Delta_\perp|^2)} \right. \\
&\quad \left. - \frac{x(1-x)q_{a\perp}q_{b\perp}^* k_{2\perp}}{\Delta_\perp^* k_{1\perp}^* (k_{1\perp} - x\Delta_\perp)} - \frac{xq_{a\perp}^* q_{b\perp} k_{1\perp}}{|\Delta_\perp|^2 (k_{1\perp}^* - x\Delta_\perp^*)} + \frac{xq_{b\perp}^* (q_{b\perp} + k_{2\perp})}{\Delta_\perp^* k_{1\perp}^*} \right]. \quad (43)
\end{aligned}$$

Next, we consider the amplitude $gg \rightarrow g\bar{q}qg$, with the production of a $\bar{q}q$ pair in the central-rapidity region (Fig.4b) [14], [17]. Using the amplitudes with a $\bar{q}q$ pair and two negative-helicity gluons [22], and the algebra (7) we obtain

$$\begin{aligned}
M^{\bar{q}q}(-p_a, -\nu_a; p_{a'}, \nu_{a'}; k_1, -\nu; k_2, \nu; p_{b'}, \nu_{b'}; -p_b, -\nu_b) & \quad (44) \\
= 4 \hat{s} \left[ig f^{aa'c} C_{-\nu_a \nu_{a'}}^{gg}(-p_a, p_{a'}) \right] \frac{1}{\hat{t}_a} \left\{ g^2 \left[(\lambda^{c'} \lambda^c)_{d_2 \bar{d}_1} A_{-\nu\nu}^{\bar{q}q}(k_1, k_2) - (\lambda^c \lambda^{c'})_{d_2 \bar{d}_1} A_{\nu-\nu}^{\bar{q}q}(k_2, k_1) \right] \right\} \\
\times \frac{1}{\hat{t}_b} \left[ig f^{bb'c'} C_{-\nu_b \nu_{b'}}^{gg}(-p_b, p_{b'}) \right],
\end{aligned}$$

with k_1 the antiquark, and the production vertex $g^* g^* \rightarrow \bar{q}q$ enclosed in curly brackets. The vertex $A^{\bar{q}q}$ is

$$\begin{aligned}
A_{+-}^{\bar{q}q}(k_1, k_2) &= - \sqrt{\frac{k_1^+}{k_2^+}} \left\{ \frac{k_2^+ |q_{b\perp}|^2}{(k_1^+ + k_2^+) \hat{s}_{12}} + \frac{k_2^- k_{2\perp} |q_{a\perp}|^2}{k_{1\perp} (k_1^- + k_2^-) \hat{s}_{12}} + \frac{k_2^+ k_{1\perp}^* (q_{b\perp} + k_{2\perp})}{k_1^+ \hat{t}} \right. \\
&\quad \left. + \frac{(q_{b\perp} + k_{2\perp}) [k_1^- k_2^+ - k_{1\perp}^* k_{2\perp} - (q_{b\perp}^* + k_{2\perp}^*) k_{2\perp}] - |k_{2\perp}|^2}{k_{1\perp} \hat{s}_{12}} - \frac{|k_{2\perp}|^2}{\hat{s}_{12}} \right\}. \quad (45)
\end{aligned}$$

As in the gluonic case, we note that the vertex $A_{+-}^{\bar{q}q}$ must be at least linear in $|q_{i\perp}|$,

$$\lim_{|q_{i\perp}| \rightarrow 0} A_{+-}^{\bar{q}q}(k_1, k_2) = O(|q_{i\perp}|) \quad (46)$$

with $i = a, b$, which is fulfilled by eq.(45). Using eq.(42), the vertex $A_{+-}^{\bar{q}q}$ may be rewritten as [14],

$$\begin{aligned}
A_{+-}^{\bar{q}q}(k_1, k_2) &= - \sqrt{\frac{1-x}{x}} \left[\frac{k_{1\perp}^* (q_{b\perp} + k_{2\perp})}{\hat{t}} + \frac{x|q_{a\perp}|^2 k_{1\perp}^* k_{2\perp}}{|\Delta_\perp|^2 (|k_{1\perp} - x\Delta_\perp|^2 + x(1-x)|\Delta_\perp|^2)} \right. \\
&\quad \left. - \frac{x(1-x)q_{a\perp}q_{b\perp}^*}{\Delta_\perp^* (k_{1\perp} - x\Delta_\perp)} + \frac{xq_{a\perp}^* q_{b\perp} k_{1\perp}^*}{|\Delta_\perp|^2 (k_{1\perp}^* - x\Delta_\perp^*)} + \frac{xq_{b\perp}^*}{\Delta_\perp^*} \right]. \quad (47)
\end{aligned}$$

In the multi-Regge limits, $k_1^+ \gg k_2^+$, i.e. for $x \rightarrow 1$, or $k_2^+ \gg k_1^+$, i.e. for $x \rightarrow 0$, the vertex (47) vanishes. In addition, in the soft limit $k_1 \rightarrow 0$, i.e. for $x \rightarrow 0$ and $k_{1\perp} \rightarrow 0$, the vertex $A_{+-}^{\bar{q}q}$ (47) has a square-root divergence,

$$\lim_{k_1 \rightarrow 0} A_{+-}^{\bar{q}q}(k_1, k_2) = \frac{1}{\sqrt{x}} \frac{xq_{a\perp}q_{b\perp}^*}{\Delta_\perp^* (k_{1\perp} - x\Delta_\perp)}, \quad (48)$$

which when integrated over the quark phase space does not yield any infrared divergence because soft quarks are infrared safe. Finally, the amplitudes of Fig. 4 with a quark in the upper and/or in the lower line are obtained via the substitution (16).

5 Conclusions

In these proceedings we have shown how the helicity formalism may be used in the high-energy limit to compute all the corrections to the tree-level FKL amplitudes induced by the corrections to the multi-Regge kinematics. The building blocks of the ensuing amplitudes are the vertices which describe the emission of two partons in the forward-rapidity region (sect. 4.1), or in the central-rapidity region (sect. 4.2). Once the parton helicities are fixed the analytic form of the vertices simplifies considerably (see ref. [12] versus ref. [13], [14] and [17]). The vertices for the emission in the central-rapidity region determine the real NLL corrections to the BFKL equation [14], and the vertices for the emission in the forward-rapidity region fix the boundary conditions to it.

Acknowledgements I wish to thank the organizers of Les Rencontres de Physique de la Vallée d'Aoste for the warm hospitality and for the support.

References

- [1] H1 Collab., Nucl. Phys. **B407**, 515 (1993); Nucl. Phys. **B439**, 471 (1995); preprint DESY 96-039;
ZEUS Collab., Phys. Lett. **B316**, 412 (1993); Zeit. Phys. **C65**, 369 (1995); Zeit. Phys. **C69**, 607 (1996).
- [2] E.A. Kuraev, L.N. Lipatov and V.S. Fadin, Zh. Eksp. Teor. Fiz. **72**, 377 (1977) [Sov. Phys. JETP **45**, 199 (1977)]; Ya.Ya. Balitsky and L.N. Lipatov, Yad. Fiz. **28** 1597 (1978) [Sov. J. Nucl. Phys. **28**, 822 (1978)].
- [3] A. Bassetto, M. Ciafaloni and G. Marchesini, Phys. Rep. **100**, 201 (1983).
- [4] S. Catani and F. Hautmann, Nucl. Phys. **B427**, 475 (1994).
- [5] A.H. Mueller, Nucl.Phys. **B** (Proc.Suppl.) **18C**, 125 (1991).
- [6] A.H. Mueller and H. Navelet, Nucl. Phys. **B282**, 727 (1987).

- [7] V. Del Duca and C.R. Schmidt, Phys. Rev. D **51**, 2150 (1995).
- [8] L.N. Lipatov, Yad. Fiz. **23**, 642 (1976) [Sov. J. Nucl. Phys. **23**, 338 (1976)].
- [9] E.A. Kuraev, L.N. Lipatov and V.S. Fadin, Zh. Eksp. Teor. Fiz. **71**, 840 (1976) [Sov. Phys. JETP **44**, 443 (1976)].
- [10] L.N. Lipatov, Nucl. Phys. **B365**, 614 (1991).
- [11] V. Del Duca, Phys. Rev. D **52**, 1527 (1995).
- [12] L.N. Lipatov and V.S. Fadin, Yad. Fiz. **50**, 1141 (1989) [Sov. J. Nucl. Phys. **50**, 712 (1989)].
- [13] V. Del Duca, preprint DESY 95-249.
- [14] V.S. Fadin and L.N. Lipatov, preprint DESY 96-020.
- [15] J.C. Collins and R.K. Ellis, Nucl. Phys. **B360**, 3 (1991);
S. Catani, M. Ciafaloni and F. Hautmann, Nucl. Phys. **B366**, 135 (1991).
- [16] V.S. Fadin and M.I. Kotsky, preprint Budker INP 95-51.
- [17] V. Del Duca, preprint Edinburgh 96/3.
- [18] M.L. Mangano and S.J. Parke, Phys. Rep. **200**, 301 (1991).
- [19] S.J. Parke and T. Taylor, Phys. Rev. Lett. **56**, 2459 (1986).
- [20] B.L. Combridge and C.J. Maxwell, Nucl. Phys. **B239**, 429 (1984).
- [21] F.A. Berends and W. Giele, Nucl. Phys. **B294**, 700 (1987);
M.L. Mangano, S.J. Parke and Z. Xu, Nucl. Phys. **B298**, 653 (1988).
- [22] M.L. Mangano and S.J. Parke, Nucl. Phys. **B299**, 673 (1988).